Spatial Delocalization in *para*-H_2 Clusters†

Eran Rabani* and Joshua Jortner*

School of Chemistry, The Sackler Faculty of Exact Sciences, Tel Aviv University, Tel Aviv 69978, Israel

Received: December 5, 2005; In Final Form: March 20, 2006

We applied the quantum path integral Monte Carlo method for the study of (*para*-H_2)$_N$ ($N = 5-33$) clusters at $T = 2$ K, exploring static and dynamic order, which originates from the effects of zero-point energy, kinetic energy, and thermal fluctuations in quantum clusters. Information on dynamic structure was inferred from the asymptotic tails of the cage correlation function calculated from the centroid Monte Carlo trajectory. The centroid cage correlation function decays to zero for large clusters ($N = 15-33$), manifesting the interchange of molecules between different solvation shells, with statistically diminishing back interchange. Further evidence for the floppiness of *para*-hydrogen clusters emerges from the Monte Carlo evolution of the centroid of a tagged molecule, which exhibits significant changes in the list of its first and second solvation shells due to the interchange of molecules between these shells.

I. Introduction

H_2 is the most ubiquitous molecule in the universe. In the ground $J = 0$ rotational state, molecular *para*-H_2 constitutes a spinless boson, which, together with the ^{4}He atom, is considered as the only naturally occurring particle whose assembly might manifest superfluidity.[1] The attainment of Bose condensation in a uniform, ideal gas of *para*-H_2 is expected to be characterized by a critical temperature $T_c = 6-8$ K,[1−3] which is consistent with an early theoretical estimate,[4] although a lower value of $T_c = 2.1$ K was inferred from later analysis.[3,5] These estimates of T_c are lower than the triple-point temperature of hydrogen in the bulk,[6] precluding the prevalence of Bose−Einstein condensation. The lowering of the "melting" temperature, i.e., the order−disorder, broadened transition temperature in a cluster relative to the corresponding infinite bulk system,[7] may be beneficial for the attainment of lower-temperature liquid *para*-hydrogen clusters, where Bose−Einstein condensation may be manifested.[4]

This problem was addressed by quantum path integral Monte Carlo simulations of *para*-H_2 clusters.[8] Sindzingre et al.[2,8,9] reported on the melting of (*para*-H_2)$_N$ clusters. For $N = 33$ and $N = 13$, the radial density profiles indicate "liquid"-type behavior above $T_M = 5$ K, while below $T = 5$ K, structural selectivity is manifested for these clusters, revealing rigid structures, e.g., a pentagonal bipyramidal core for $N = 33$ and an icosahedral structure for $N = 13$. Raman spectroscopy in cryogenically cooled free jets provides significant information on the identification of small (*para*-H_2)$_N$ ($N = 2\cdots8$) clusters.[10] For (*para*-H_2)$_N$ ($N = 13$ and 33) clusters, liquid clusters appeared early in the expansion. A larger cluster ($N > 55$) at lower source temperatures and larger source pressures underwent a transition to the solid configuration,[10] with the coexistence between solid and liquid. Raman peaks suggest that these large, predominantly solid clusters have a significant liquid fraction, which is possibly located at the surface.[10] Early attempts to calculate Raman spectral shifts assuming a rigid structure for these cluster were unsuccessful.[11] The good agreement that was accomplished between experimental and model calculations, using pair distribution functions for the individual clusters, indicates that these clusters are nonrigid and floppy.[10,12] However, direct evidence for cluster floppiness and particle delocalization in these quantum clusters is not yet available.

In this paper, we applied the quantum path integral Monte Carlo (PIMC) method[12,13] for the study of (*para*-H_2)$_N$ ($N = 5-33$) clusters. To address the issue of floppiness, namely, are the cluster solid or liquid like, we calculated the cage correlation functions to describe the change in the molecular surrounding.[14−16] In this context, the interesting issue is whether particles diffuse or not, and the cage correlation function is an extremely useful tool to address this issue for finite small systems.

As we consider the intermolecular pair−centroid distances, the effects of exchange interactions, which originate from boson permutation symmetry, will be of minor importance. Our treatment of a cluster of particles that obey Boltzmann statistics provides evidence for the highly delocalized nature of these finite systems, despite the fact that boson permutation symmetry has been neglected. Thus, spatial delocalization can originate from zero-point energy and kinetic energy effects and the inclusion of the proper Bose statistics can probably enhance, but not suppress delocalization in these quantum clusters.

II. Model and Theory

In this section, we describe the model used to study the structural properties of small clusters of *para*-hydrogen, provide some technical details regarding the path-integral Monte Carlo (PIMC) approach used, and describe the approach we adopt to study the change in atomic surroundings of these quantum clusters.

A. Model Potential. The model potential we used to study small *para*-hydrogen clusters is based on the Silvera−Goldman two-body potential,[17,18] where the entire H_2 molecule is described as a spherical particle, so the potential depends only on the radial distance between the molecules. It has been developed to study the properties of condensed hydrogen and has been used in this context to explain the thermodynamic properties and the phase equilibrium of clusters and liquid hydrogen,[19−25] as well as dynamical properties of liquid

† Part of the special issue "Robert J. Silbey Festschrift".

* Corresponding authors. E-mail: rabani@tau.ac.il (E.R.); jortner@chemsgr1.tau.ac.il (J.J.).

10.1021/jp057067z CCC: $33.50
Published on Web 04/21/2006

TABLE 1: Parameters of the Silvera−Goldman Model Potential for *para*-Hydrogen in Atomic Units

α	δ	γ	C_6	C_8	C_9	C_{10}	r_c
1.713	1.5671	0.00993	12.14	215.2	143.1	4813.9	8.321

hydrogen and deuterium.[26−39] The Silvera−Goldman potential is given by

$$V(r) = \exp(\alpha - \delta r - \gamma r^2) - \left(\frac{C_6}{r^6} + \frac{C_8}{r^8} + \frac{C_{10}}{r^{10}}\right) f_c(r) + \frac{C_9}{r^9} f_c(r) \quad (1)$$

where the first term on the right-hand side (RHS) accounts for short-range repulsion interactions, the second set of terms on the RHS account for long-range attractive dispersion interactions, and the last term on the RHS is an effective three-body correction.[17] The last two terms are multiplied by a damping function, which turns off these interactions at short distances, and is given by

$$f_c(r) = e^{-(r_c/r - 1)^2}\theta(r_c - r) + \theta(r - r_c) \quad (2)$$

where $\theta(r)$ is the Heaviside function (step function). The parameters for the potential are given in Table 1.

B. Path Integral Monte Carlo Approach. The calculation of the static structural properties of *para*-hydrogen clusters were based on the PIMC approach described in ref 13. For reasons discussed above, our simulations do not include exchange of particles and, thus, are exact only in the limit of Boltzmann statistics.

The path integral method is based on the evaluation of the many-body density matrix, $\hat{\rho}_\beta = \exp\{-\beta\hat{H}\}$, where $\beta = (1/k_B T)$ is the inverse temperature and $\hat{H}$ is the many-body Hamiltonian given by (from now on we assume atomic units where p = 1):

$$\hat{H} = -\frac{1}{2m}\sum_{i=1}^{N} \nabla_i^2 + \sum_{i>j}^{N} \hat{V}(r_{ij}) \quad (3)$$

As before, the entire H_2 molecule was described as a spherical particle with mass m and the two-body interaction potential $\hat{V}(r_{ij})$ between particles i and j at distance $r_{ij} = |\boldsymbol{r}_i - \boldsymbol{r}_j|$ is given by eq 1.

The density matrix described above is the starting point for evaluation of expectation values of an arbitrary observable:

$$\langle\hat{A}\rangle = Z^{-1} Tr \hat{\rho}_\beta \hat{A} = Z^{-1}\int dR\, dR' \rho_\beta(R, R') A(R', R) \quad (4)$$

where $R = \{\boldsymbol{r}_1 \cdots \boldsymbol{r}_N\}$ is a shorthand notation for the position vector of all particles, $\rho_\beta(R, R') = \langle R|\hat{\rho}_\beta|R'\rangle$, $A(R, R') = \langle R|\hat{A}|R'\rangle$, and $Z = Tr \exp\{-\beta\hat{H}\}$ is the partition function. If the operator $\hat{A}$ depends only on the position of all particles, i.e., it is diagonal in the coordinate representation, eq 4 takes a simpler form given by:

$$\langle\hat{A}\rangle = Z^{-1}\int dR \rho_\beta(R, R) A(R) \quad (5)$$

We now rewrite the density matrix in terms of a product of high-temperature density matrixes. This is required to transform eq 5 to a form suitable for Monte Carlo techniques:

$$\hat{\rho}_\beta = \exp\{-\beta\hat{H}\} = (\exp\{-\epsilon\hat{H}\})^P \equiv \hat{\rho}_\epsilon^{\,P} \quad (6)$$

where $\epsilon = \beta/P$. By inserting a complete set of position states between the high-temperature density matrixes, we can obtain our working expression for the expectation value of the observable under consideration:

$$\langle\hat{A}\rangle = Z^{-1}\int dR_1 \cdots dR_P \rho_\epsilon(R_1, R_2)\rho_\epsilon(R_2, R_3)\cdots\rho_\epsilon(R_P, R_1)A(R_P) \quad (7)$$

where $\rho_\epsilon(R, R') = \langle R|\hat{\rho}_\epsilon|R'\rangle = \langle R|\exp\{-\epsilon\hat{H}\}|R'\rangle$ is the matrix element of the high-temperature density matrix.

In this work, we used the pair product approximation to evaluate the high-temperature density matrix.[13] This approximation reduces the number P of slices required to converge the full density matrix as compared to the widely used primitive approximation. The two different approximations yield similar results for several cluster sizes within the noise level of the PIMC simulations. The pair-product approximation for the high-temperature density matrix is given by:

$$\rho_\epsilon(R, R') \propto \exp\left\{-\frac{m}{2\epsilon}\sum_{i=1}^{N}(\boldsymbol{r}_i - \boldsymbol{r}_i')^2 - \sum_{i>j}^{N} u(\boldsymbol{r}_{ij}, \boldsymbol{r}_{ij}'; \epsilon)\right\} \quad (8)$$

where $\boldsymbol{r}_{ij} = \boldsymbol{r}_i - \boldsymbol{r}_j$ and $u(\boldsymbol{r}, \boldsymbol{r}'; \epsilon)$ is the exact action for a pair of hydrogen molecules (described each by a spherical particle) given by

$$u(\boldsymbol{r}, \boldsymbol{r}'; \epsilon) = -\log\left\{\frac{\rho_p(\boldsymbol{r}, \boldsymbol{r}'; \epsilon)}{\rho_p^{\,0}(\boldsymbol{r}, \boldsymbol{r}'; \epsilon)}\right\} \quad (9)$$

In the above equation, $\rho_p(\boldsymbol{r}, \boldsymbol{r}'; \epsilon)$ is the relative pair density matrix of two hydrogen molecules, and $\rho_p^{\,0}(\boldsymbol{r}, \boldsymbol{r}'; \epsilon)$ is the corresponding relative free-particle pair density matrix. These are given by:

$$\rho_p(\boldsymbol{r}, \boldsymbol{r}'; \epsilon) = \sum_n \phi_n^*(\boldsymbol{r})\phi_n(\boldsymbol{r}')\exp\{-\epsilon E_n\} \quad (10)$$

and

$$\rho_p^{\,0}(\boldsymbol{r}, \boldsymbol{r}'; \epsilon) = \sum_n \phi_n^0 *(\boldsymbol{r})\phi_n^{\,0}(\boldsymbol{r}')\exp\{-\epsilon E_n^{\,0}\} \quad (11)$$

respectively. In the above equations, ϕ_n and E_n are the eigenstates and eigenvalues of the relative Schroedinger equation for a pair of *para*-hydrogen molecules, and ϕ_n^0 and E_n^0 are the corresponding quantities when the interactions between the pair of *para*-hydrogen molecules is turned off.

C. Modeling the Change in Atomic Surroundings. One of the major goals of the present study is related to the issue of mobility of hydrogen molecules in the cluster. In other words, is the surrounding of each hydrogen molecule static or dynamic, and does this property vary with system size? The answer to this question cannot be obtained from static information such as the pair distribution function. In classical disordered systems, a valuable approach to address this question is based on the cage correlation function,[14−16] which provides an accurate measure of changes in the molecule's surroundings. Application of the cage correlation function to extract the change in the surroundings in classical systems can be obtained from either Monte Carlo or molecular dynamics trajectories. In such systems, it is found that for solids the cage correlation function does not decay at long times, while for liquids, an exponential decay is observed at long time.[14]

Here, we adopt this approach and apply the analysis based on the cage correlation function to the Monte Carlo dynamics of the centroid (center of mass of the beads) of each molecule. To calculate this correlation function for *para*-hydrogen clusters,

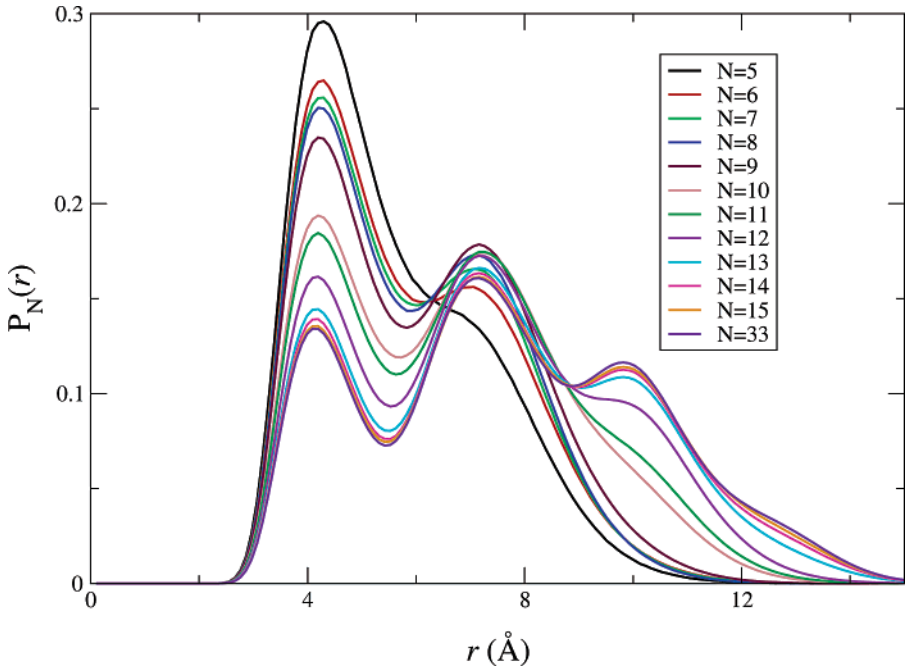

Figure 1. Radial pair distribution functions, $P_N(r)$, for *para*-hydrogen clusters of different size. All distributions are normalized to $\int_0^\infty P_N(r)\,dr = 1$.

we generate a Monte Carlo trajectory of the centroid of all molecules in the cluster using the PIMC method described above and carry out the calculation of the cage correlation function for each trajectory.

The cage correlation function is based on introducing a generalized neighbor list (l_i) for molecule i in an N molecule system. This list is a vector of length N, and is defined as

$$l_i \equiv \begin{pmatrix} f(r_{i1}^c) \\ \vdots \\ f(r_{iN}^c) \end{pmatrix} \tag{12}$$

where $f(r_{ij}^c)$ is a function of the intermolecular centroid distance (r_{ij}^c) and is taken to be the Heaviside function,

$$f(r_{ij}^c) = \theta(r_{nlist}^c - r_{ij}^c) = \begin{cases} 1 & \text{if } r_{ij}^c \le r_{nlist}^c \\ 0 & \text{otherwise} \end{cases} \tag{13}$$

where r_{nlist}^c is the centroid neighbor list cutoff radius taken to be at the location of the first minimum in the pair correlation function. The centroid cage correlation function is defined using the generalized neighbor list, l_i, as

$$C_l(t) \equiv \frac{\langle l_i(0) \cdot l_i(t) \rangle}{\langle l_i(0)^2 \rangle} \tag{14}$$

where t is the Monte Carlo step. The properties of the cage correlation function for classical fluids has been described in detail elsewhere.[14−16] In brief, if the surroundings of a molecule are static, the cage correlation function will decay to a plateau due to the vibrational motion. When the surroundings change, the fast decay to the plateau will be followed by a longer time decay associated with the change in the surroundings of the molecule. Below, we use this correlation function to study the quantum fluctuations of the surroundings of hydrogen molecules in small cluster.

D. Computations. We have performed PIMC simulations for several $(para\text{-}H_2)_N$ clusters in the size domain from $N = 5$ to $N = 33$ at $T = 2$ K. The staging algorithm[40] for Monte Carlo chain moves was employed to compute the numerically exact static information and the centroid Monte Carlo trajectory required to obtain the centroid cage correlation function. The imaginary time interval was discretized into P slices of size $\epsilon = \beta/P$ with $P = 30$. 3×10^6 Monte Carlo passes were made, each pass consisted of attempting moves in all molecules and all the beads that were staged. The acceptance ratio was set to be approximately 0.25 for the staging moves, which required 5−10 staging beads, depending on the system size. Following the staging moves, to accelerate the sampling of configuration space, we have added single-particle centroid moves. These moves consist of an attempt to displace the center of mass of the beads of each particle in a random direction. Such a move was accepted with the standard Metropolis criteria. The magnitude of the displacement was set to obtain an acceptance ratio of 0.25 for this move.

III. Results

In Figure 1, we plot the pair distribution function, $P_N(r)$, for *para*-H_2 clusters of varying size. This set of clusters was also studied recently by Tejeda et al. using the diffusion Monte Carlo (DMC) method at zero temperature.[10] The pair distribution function calculated using the PIMC method at $T = 2$ K is qualitatively very similar to that obtained using the DMC approach. The common features are the position and height of the first peak in $P_N(r)$ and the development of the shoulders into a second and a third solvation peak as the cluster size is increased. The differences are mainly associated with the relative magnitude of the solvation peaks. These can result from the effect of thermal fluctuations (relative to the quantum fluctuations), even at $T = 2$ K, and from the fact that different interacting pair-potentials were used in the studies. We believe that Bose statistics may also contribute to this difference; however, we would like to point out that, for liquid helium, Bose statics have a negligible effects on $P_N(r)$, even below the λ transition.[41]

One of the major conclusions drawn from the work of Tejeda et al.[10] is that the shape of the pair correlation function, which

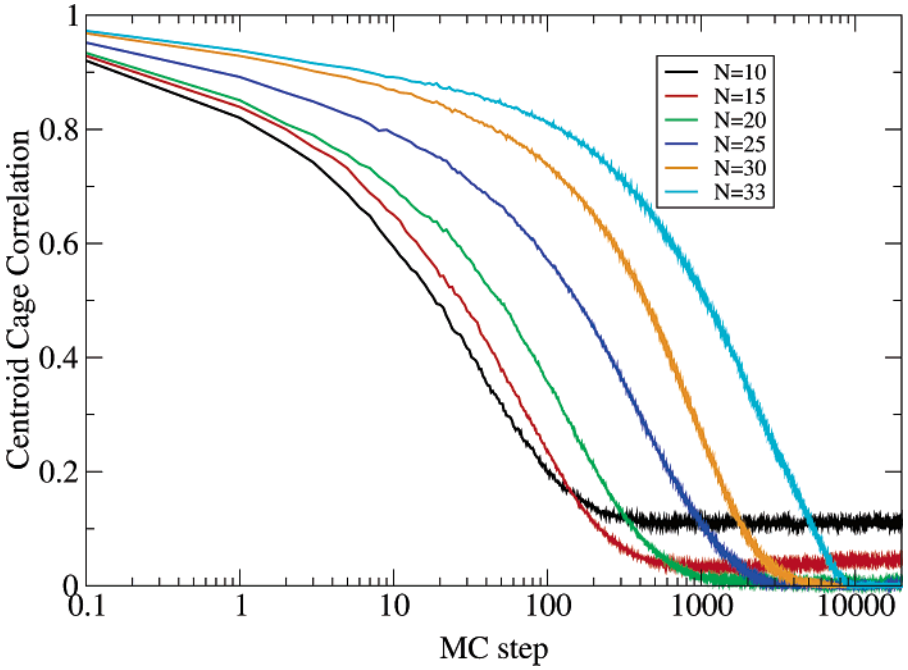

Figure 2. Plot of the centroid cage correlation computed for *para*-hydrogen clusters at different cluster size.

resembles that of bulk liquid,[19] indicates that the *para*-hydrogen cluster is highly delocalized and floppy. Of course, the pair distribution function provides only an indirect measure of delocalization, and for small cluster sizes, it is probably not a very good indirect measure. In fact, for smaller clusters where a second solvation shell has not developed, the difference between the pair distribution function of a floppy versus a rigid cluster is not noticeable, and even for a larger cluster where a second solvation peak appears, it is very difficult to determine whether the cluster is floppy or rigid based on the pair distribution function alone.

A more decisive picture emerges from the analysis shown in Figure 2, where we plot the centroid cage correlation function obtained from the Monte Carlo centroid trajectories for a subset of *para*-H_2 clusters (i.e., $N = 10, 15, 20, 25, 30, 33$). We would like to note that this correlation function cannot be used to infer information about the real-time dynamics of these systems. However, it does provide a clear-cut evidence for the floppiness and particle delocalization in these clusters because we expect the centroid cage correlation function to decay to zero for floppy clusters, even if the trajectory is generated using the Monte Carlo method.

As can be seen in Figure 2, for larger *para*-H_2 clusters ($N > 15$), indeed, the centroid cage correlation function decays to zero. This can be understood only if each molecule loses its original surrounding molecules at long Monte Carlo time. In contrast, for the smaller clusters ($N = 10-15$), the centroid cage correlation does not decay to zero at large Monte Carlo time, but rather decays to a small plateau. The appearance of this finite size plateau is a result of the fact that the definition of the generalized neighbor list, l_i, does not constitute a sensitive probe when the clusters are small when nearly all atoms reside within the first solvation shell of each other.

A closer examination of individual centroid Monte Carlo trajectories for the smaller clusters (not shown here) reveals that they are indeed floppy. For example, we followed the Monte Carlo evolution of the centroid of a tagged molecule and found significant changes in the list of its first and second solvation shells. Specifically, we find that, occasionally, a molecule from its first solvation shell pops out to the second solvation shell and, in return, a molecule from the second solvation shell pops in to the first solvation shell. Because the cluster is small, this process occurs also in the back direction, while for larger clusters, the probability that the same two molecules will re-interchange solvation shells is quite small.

This particle interchange process results in a decay of the centroid cage correlation function at intermediate Monte Carlo times. When the back interchange is blocked for statistical reasons, the centroid cage correlation function decays to zero. However, for small cluster, this back interchange occurs with a finite probability, and indeed, the centroid cage correlation function decays to a finite plateau at long Monte Carlo times. The height of the plateau is a direct measure of the probability for this back interchange. As can be seen in Figure 2, the value of the plateau decreases with increasing cluster size, approaching zero for large clusters.

IV. Conclusions and Discussion

The quantum path integral Monte Carlo method provided information on cluster floppiness and particle delocalization in *para*-hydrogen clusters at $T = 2$ K, which originate from the effects of zero-point energy, kinetic energy, and thermal fluctuations. Of considerable interest is the static and dynamic structure of these quantum clusters. Regarding the static structure, the pair distribution function at $T = 2$ K exhibits solvation peaks, which manifest both quantum fluctuations and thermal fluctuations at this finite, low temperature. Information on dynamic structure of *para*-hydrogen clusters was inferred from the asymptotic tails of the cage correlation function, calculated from the centroid Monte Carlo trajectory. The decay of the centroid cage correlation function to zero for large clusters ($N = 15-33$) manifests the interchange of molecules between different solvation shells, with statistically diminishing back interchange. This analysis of the cage correlation function provides new information on the floppiness of *para*-hydrogen quantum clusters that is supported by the Monte Carlo evolution of the centroid of a tagged molecule to interrogate changes in its list in different shells. The extension of the analysis of the cage correlation function from classical fluids to quantum

clusters will be of considerable interest for the exploration of the structure of dislocations in low-temperature solid *para*-hydrogen and of ^{4}He, which are of considerable current interest in the context of probable Bose−Einstein condensation in these solids.[42−45] The methods advanced herein will be useful for the understanding of the dynamic structure of lattice vacancies in these quantum solids, while Bose condensation has to be explored by incorporating quantum exchange effects.[13]

Acknowledgment. We wish to thank Professor J. Peter Toennies for stimulating discussions. This work was supported by The Israel Science Foundation (grant no. 31/02-1 to E.R.) and by Binational German−Israeli James Frank Program on Laser−Matter Interactions (to J.J).

References and Notes

(1) Ginzburg, V. L.; Sobyanin, A. A. *JETP Lett.* **1972**, *15*, 242.
(2) Ceperley, D. M.; Manousakis, E. *J. Chem. Phys.* **2001**, *115*, 10111.
(3) Apenko, C. M. *Phys. Rev. B* **1999**, *60*, 3052.
(4) Aculichev, A.; Bulanov, V. A. *JETP Lett.* **1974**, *38*, 329.
(5) Vorobev, V. S.; Malyshenko, P. J. *J. Phys. Condens. Matter* **2000**, *12*, 5071.
(6) Maris, H. J.; Seidel, G. M.; Williams, F. I. B. *Phys. Rev. B* **1987**, *36*, 6799.
(7) Berry, R. S. In *Theory of Atomic and Molecular Clusters*; Jellinek, J., Ed.; Springer-Verlag: Berlin, 1999.
(8) Sindzingre, P.; Ceperley, D. M.; Klein, M. L. *Phys. Rev. Lett.* **1991**, *67*, 1871.
(9) Gordillo, M.; Ceperley, D. M. *Phys. Rev. Lett.* **1997**, *90*, 3010.
(10) Tejeda, G.; Fernández, J. M.; Montero, S.; Blume, D.; Toennies, J. P. *Phys. Rev. Lett.* **2004**, *92*, 223401.
(11) Scharf, D.; Klein, M. L.; Martyna, G. *J. Chem. Phys.* **1992**, *97*, 3590.
(12) Berne, B. J.; Thirumalai, D. *Annu. Rev. Phys. Chem.* **1986**, *37*, 401.
(13) Ceperley, D. M. *Rev. Mod. Phys.* **1995**, *67*, 279.
(14) Rabani, E.; Gezelter, J. D.; Berne, B. J. *J. Chem. Phys.* **1997**, *107*, 6867.
(15) Gezelter, J. D.; Rabani, E.; Berne, B. J. *J. Chem. Phys.* **1999**, *110*, 3444.
(16) Rabani, E.; Gezelter, J. D.; Berne, B. J. *Phys. Rev. Lett.* **1999**, *82*, 3649.
(17) Silvera, I. F.; Goldman, V. V. *J. Chem. Phys.* **1978**, *69*, 4209.
(18) Silvera, I. F. *Rev. Mod. Phys.* **1980**, *52*, 393.
(19) Scharf, D.; Martyna, G.; Klein, M. L. *J. Low Temp. Phys.* **1993**, *19*, 365.
(20) Whaley, K. B. *Int. Rev. Phys. Chem.* **1994**, *13*, 41.
(21) McMahon, M. A.; Whaley, K. B. *Chem. Phys.* **1994**, *182*, 119.
(22) Chakravarty, C. *Mol. Phys.* **1995**, *84*, 845.
(23) Wang, Q.; Johnson, J. K.; Broughton, J. Q. *Mol. Phys.* **1996**, *89*, 1105.
(24) Zoppi, M.; Neumann, M.; Celli, M. *Phys. Rev. B: Condens. Matter* **2002**, *65*, 092204.
(25) Kwon, Y.; Whaley, K. B. *Phys. Rev. Lett.* **2002**, *89*, 273401.
(26) Cao, J.; Martyna, G. J. *J. Chem. Phys.* **1996**, *104*, 2028.
(27) Pavese, M.; Voth, G. A. *Chem. Phys. Lett.* **1996**, *249*, 231.
(28) Kinugawa, K. *Chem. Phys. Lett.* **1998**, *292*, 454.
(29) Bermejo, F. J.; Kinugawa, K.; Cabrillo, C.; Bennington, S. M.; Fak, B.; Fernandez-Diaz, M. T.; Verkerk, P.; Dawidowski, J.; Fernandez-Perea, R. *Phys. Rev. Lett.* **2000**, *84*, 5359.
(30) Reichman, D. R.; Rabani, E. *Phys. Rev. Lett.* **2001**, *87*, 265702.
(31) Rabani, E.; Reichman, D. R.; Krilov, G.; Berne, B. J. *Proc. Natl. Acad. Sci. U.S.A.* **2002**, *99*, 1129.
(32) Rabani, E.; Reichman, D. R. *Europhys. Lett.* **2002**, *60*, 656.
(33) Rabani, E.; Reichman, D. R. *Phys. Rev. E* **2002**, *65*, 036111.
(34) Rabani, E.; Reichman, D. R. *J. Chem. Phys.* **2002**, *116*, 6271.
(35) Reichman, D. R.; Rabani, E. *J. Chem. Phys.* **2002**, *116*, 6279.
(36) Rabani, E.; Reichman, D. R. *J. Chem. Phys.* **2004**, *120*, 1458.
(37) Rabani, E.; Reichman, D. R. *Annu. Rev. Phys. Chem.* **2005**, *56*, 157.
(38) Hone, T. D.; Voth, G. A. *J. Chem. Phys.* **2004**, *121*, 6412.
(39) Poulsen, J. A.; Nyman, G.; Rossky, P. J. *J. Phys. Chem. B* **2004**, *108*, 19799.
(40) Pollock, E. L.; Ceperley, D. M. *Phys. Rev. B* **1984**, *30*, 2555.
(41) Rabani, E. Unpublished.
(42) Leggett, A. J. *Phys. Rev. Lett.* **1970**, *25*, 1543.
(43) Levy, B. G. *Phys. Today* **2004**, *April*, 21.
(44) Kim, E. S.; Chan, M. H. W. *Nature* **2004**, *247*, 225.
(45) Jortner, J.; Rosenblit, M. *Adv. Chem. Phys.* **2006**, *132*, 247.